The Generalized Droop Model for Submarine Fiber-optic Systems

The Generalized Droop Model for Submarine Fiber-optic Systems

Alberto Bononi, *Senior Member, IEEE,* Jean-Christophe Antona, Paolo Serena, *Member, IEEE*, Alexis Carbo-Meseguer, and Chiara Lasagni, *Student Member, IEEE*

(Invited Paper)

***Abstract*—We review the fundamentals of the recently proposed Generalized Droop model and highlight its use in power efficiency optimization of long-haul low-SNR space-division multiplexed submarine links.**

***Index Terms*—Optical Communications, Optical amplifiers, Submarine transmission, Signal Droop.**

I. Introduction

Optical amplifiers in submarine links are normally operated in constant output power (COP) mode [1]. The capacity of COP submarine links is limited because of the maximum end-to-end electrical voltage used to feed the amplifiers laser pumps from the shores [2], which in turn implies a limit on the per-amplifier optical pump power, and thus a limit on the available amplifier total optical output power (often called saturation power) [3]. This is the major reason why next generation submarine links will use space division multiplexing (SDM) [4] to make the best use of the available amplifiers power, and thus in turn of the available signal power [5]–[8]. The reason is readily understood from the Shannon capacity of the link

$$C = N_m N_c B_c 2 \log_2(1 + \Gamma\, SNR) \tag{1}$$

where: N_m is the number of spatial modes (i.e., parallel 2-polarization single-mode fibers in a first implementation [9], [10], or cores in multicore fibers (MCF) in a second phase [11]–[13]); N_c the number of wavelength division multiplexed (WDM) channels of bandwidth B_c on each mode; SNR their received signal to noise ratio; and $\Gamma < 1$ is an implementation SNR-penalty called *gap to capacity*. Capacity formula (1) assumes the additive Gaussian mode/wavelength channels are identical and independent, i.e., there is no multi-input multi-output processing at the receiver [14].

From (1) we easily see that instead of logarithmically increasing C by increasing signal power/SNR, it is more power-efficient to increase C by linearly increasing the number of parallel channels $N_m N_c$ [15], [16], by increasing the SDM channels and enlarging the occupied bandwidth [11].

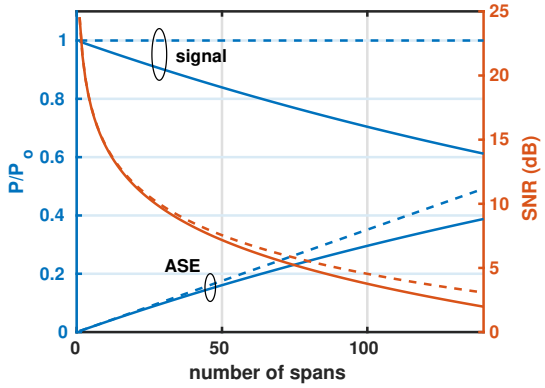

Figure 1. Signal power and accumulated ASE power at amplifier output normalized to amplifier total output power P_o (left axis) and SNR (right axis) versus number of crossed amplifiers (i.e., spans). Solid lines: COP link, Dashed lines: CG link. Ratio of total amplifier input power to total equivalent-power of ASE generated at the amplifier: $SNR_1 = 24.5$dB . Note that, for any SNR_1, the SNR gap between CG and COP links becomes important only at SNR below 6-7 dB .

Therefore future generation submarine SDM links will likely work at powers on each spatial-mode several dB lower than the nonlinear-SNR maximizing power [7], [10], such that fiber nonlinear interference (NLI) will be of minor concern [7], [8], [17], and amplified spontaneous emission (ASE) noise will be the dominant impairment, with the modal crosstalk (XT) in MCF [12], [13], [18] and the guided acoustic-wave Brillouin scattering (GAWBS) noise [19]–[21] in each spatial mode being other relevant impairments [22], [23].

It was recently shown that in the low-SNR regime envisaged for future long-haul SDM submarine COP links the standard inverse-of-sum-of-inverses accumulation rule valid for the generalized-SNR (GSNR) [24], [25], [26, eq. (8)] in links with constant gain (CG) amplifiers (hereafter referred to as CG links) ceases to be accurate [5], [6], and a new accumulation rule, known as the generalized-droop (GD) formula, applies [22], [26]–[31]. The physical reason is the existence of a gain decrease (a.k.a. *droop* [5], [6]) at each amplifier triggered by i) the local injection of ASE (and other noises such as XT/GAWBS) and ii) the COP amplifying mode [3].

As an example, Fig. 1 illustrates the effect of gain droop in a link with amplifier saturation power P_o on both the

Manuscript received xxxxxxxxx xx, xxxx; accepted xxxxxxxxx xx, xxxx. Date of publication xxxxxxxxx xx, xxxx; date of current version xxxxxxxxx xx, xxxx.

A. Bononi, P. Serena, C. Lasagni are with the Dipartimento di Ingegneria e Architettura, Università di Parma, Parma 43124, Italy (corresponding author e-mail: alberto.bononi@unipr.it). J.-C. Antona and A. Carbo-Meseguer are with Alcatel Submarine Networks, Villarceaux, France.

Color versions of one or more of the figures in this paper are available online at http://ieeexplore.ieee.org.

Digital Object Identifier xx.xxxx/JLT.xxxx.xxxxxxx.

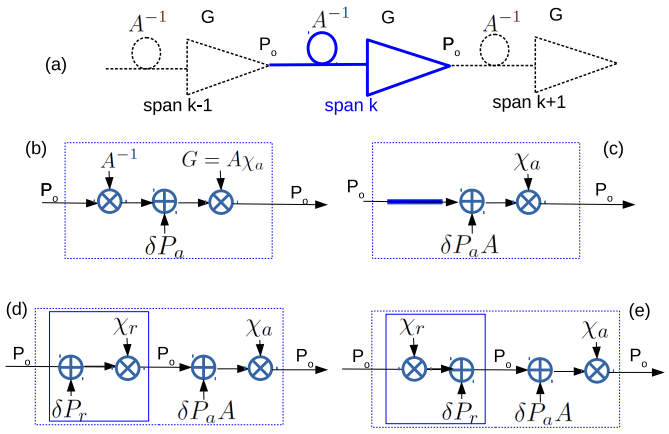

Figure 2. (a) Generic span k of an SDM submarine link with end-span COP amplifier; (b) Span power diagram; (c) Equivalent diagram with loss factored out, and ideal fiber (thick line); (d) ideal fiber in (c) replaced by an add-and-attenuate block; (e) ideal fiber in (c) replaced by an attenuate-and-add block. P_o: repeater output power (on all modes); $A > 1$: span loss; χ_a: addition droop; χ_r: redistribution droop.

useful signal and the accumulated ASE power as we increase the number of crossed amplifiers, both in a COP link (solid lines) and in a CG link (dashed lines). In the COP link the accumulated ASE power grows at the expense of the signal power. In the figure, the gap in SNR between the CG link (i.e., the GSNR) and the COP link exceeds 0.5dB at GSNRs below 6 dB (Cfr [29, Fig. 6]). Hence, although gain droop has been known for a long time [3], it becomes of much greater concern in modern low-SNR SDM links, which can properly work thanks to coherent detection and powerful error correction [6].

The GD formula has been extensively tested for low-SNR submarine SDM links and compared to experimental results with proved good accuracy [23], [31]–[34]. This paper will review the analytical model underlying the GD formula [28]–[31] and show its use in the optimization of SDM submarine links.

The paper is organized as follows. Sec. II derives the GD model and its cascading rule, and explains the minor differences between the two derivations in [29] and [31]. Sec. III shows that the GD cascading rule leads to a *disaggregation of SNR effects* different than the one routinely used for the GSNR. Sec. IV derives a new simplified expression of the COP-GD formula, i.e., the GD SNR formula when not all the amplifier bandwidth is occupied by signals. Sec. V derives several new results from the GD formula applicable to optimization of power efficiency of submarine SDM links. Finally Sec. VI summarizes our findings. The Appendices contain all the detailed derivations of the new results in the main text.

This paper is an extended version of the invited conference paper [37].

II. Generalized Droop model

Fig. 2(a) shows the considered physical SDM COP link made of N_s identical spans with span loss $A > 1$ and end-span frequency-flat amplifier with gain G and COP P_o. The generic span power flow diagram is shown in Fig. 2(b). Here

$$\delta P_a = N_m h f_0 B_a F \tag{2}$$

is the amplifier-input equivalent ASE power generated inside the N_m-mode amplifier of bandwidth $B_a \equiv N_a B_c$, with N_a the number of ASE-occupied slots of bandwidth B_c, F the frequency-flat noise figure, h Planck's constant and f_0 the WDM central frequency, and $\chi_a < 1$ is the net span gain, also called the ASE(-induced) gain-droop. Fig. 2(c) shows an equivalent block diagram where span loss is "factored-out". Droop exists because of the COP constraint, which from Fig. 2 (c) reads as: $(P_o + \delta P_a A)\chi_a = P_o$ and yields the ASE gain-droop expression

$$\chi_a = (1 + SNR_{1a}^{-1})^{-1} \tag{3}$$

where we defined

$$SNR_{1a} \triangleq \frac{P_o/A}{\delta P_a} \tag{4}$$

as the ratio of total amplifier input power to total equivalent-power of ASE generated at the amplifier. Once fiber loss is factored out, the fiber becomes an identity block, indicated by a thick line in Fig. 2(c). Indeed several power-conserving noise processes (such as NLI, XT and GAWBS) may take place during fiber propagation, causing a rearrangement of power at a constant total power P_o. To account for them, Fig. 2(d) replaces the identity block by an input sub-block where first a rearrangement perturbation δP_r is added to P_o and then multiplication by a rearrangement droop $\chi_r < 1$ re-scales the sum to P_o, thus conserving power at each span. From diagram (d) the power-conservation constraint is: $(P_o + \delta P_r)\chi_r = P_o$, which yields [29]:

$$\chi_r = (1 + \frac{\delta P_r}{P_o})^{-1}. \tag{5}$$

An alternative choice is shown in diagram (e), where one first attenuates P_o by χ_r and then adds the perturbation δP_r, getting instead [28], [30], [31]:

$$\chi_r = (1 - \frac{\delta P_r}{P_o}). \tag{6}$$

Let's define the SNR degraded by δP_r generated in a single fiber span as

$$SNR_{1r} \triangleq \frac{P_o}{\delta P_r}. \tag{7}$$

Since this ratio is normally large (> 30dB), in practice diagrams (d) and (e) yield the same numerical results. However, in diagram (d) the rearrangement block is identical to the amplifier block, which leads to a more elegant SNR expression. In both diagrams (d) and (e) the net span gain (i.e., droop) is $\chi = \chi_r \chi_a$.

In the COP link, the received (RX) signal power after N_s identical spans is $P_s(N_s) = P_o \chi^{N_s}$, and by the COP constraint the RX ASE plus rearrangement noise power is $P_a(N_s) + P_r(N_s) = P_o(1 - \chi^{N_s})$. Hence the GD formula

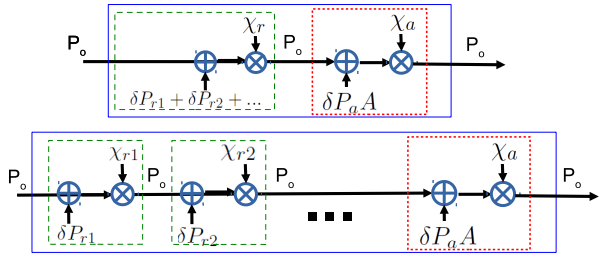

Figure 3. (Top) Span block diagram with multiple rearrangement sources. (Bottom) quasi-equivalent scheme where each source has its own COP rearrangement block.

for the RX SNR is (from now on we will use diagram (d)) $SNR = P_s(N_s)/(P_a(N_s) + P_r(N_s))$, or explicitly:

$$SNR = \frac{1}{[(1 + SNR_{1a}^{-1})(1 + SNR_{1r}^{-1})]^{N_s} - 1}. \tag{8}$$

For example, the signal power, ASE power and SNR curves in Fig. 1 were obtained by the above formulas when only ASE is present and $SNR_1 \equiv SNR_{1a} = 24.5$dB.

As long as power, gain and noise figure are uniform over frequency and modes, and all amplifier modes/channels are populated by signals (i.e., $N_a = N_c$), the GD-SNR (8) is also the per-channel RX SNR. The GD formula can be generalized to non-homogeneous links by the following cascading rule [27], [29]:

$$1 + SNR^{-1} = \prod_{k=1}^{N_s} \left(1 + SNR_{1ak}^{-1}\right)\left(1 + SNR_{1rk}^{-1}\right) \tag{9}$$

and in the "large SNR" regime where we can approximate the above product as $1 + \sum_{k=1}^{N}(SNR_{1ak}^{-1} + SNR_{1rk}^{-1})$ we retrieve the standard SNR cascading formula for CG links.

III. Disaggregation of Effects

Fig. 3(top) shows the span block diagram according to the GD model in case that a few rearrangement perturbations $r_1, r_2, ...$ (such as NLI, GAWBS and XT) are simultaneously present and add up in the rearrangement block. A numerically essentially equivalent scheme is that of the bottom diagram, where we insert a COP rearrangement block for each perturbation. The equivalence is justified by the following tight upper-bound

$$\underbrace{1 + \frac{\delta P_{r1} + \delta P_{r2} + ...}{P_o}}_{\chi_r^{-1}} \lesssim \underbrace{(1 + \frac{\delta P_{r1}}{P_o})}_{\chi_{r1}^{-1}}\underbrace{(1 + \frac{\delta P_{r2}}{P_o})}_{\chi_{r2}^{-1}} ... \tag{10}$$

since the ratios $P_o/\delta P_{ri}$ are normally large (> 30dB). The bottom scheme is however more revealing, since then the concatenation of all spans block diagrams in a COP line yields a total line block diagram that is *independent of the order of collected effects*. Mathematically, with the bottom scheme, the span k inverse rearrangement droop χ_{rk}^{-1} is the product of the droops of the individual effects:

$$\left(1 + SNR_{1rk}^{-1}\right) = \left(1 + SNR_{1r1k}^{-1}\right)\left(1 + SNR_{1r2k}^{-1}\right) \cdot \ldots$$

and thus the end-to-end inverse gain droop after N_s spans is obtained from the GD cascading rule (9) as [26, eq. (10)]:

$$\begin{aligned} 1 + SNR^{-1} &= \prod_{k=1}^{N_s}\left(1 + SNR_{1ak}^{-1}\right) \cdot \\ &\cdot \prod_{k=1}^{N_s}\left(1 + SNR_{1r1k}^{-1}\right)\prod_{k=1}^{N_s}\left(1 + SNR_{1r2k}^{-1}\right) \cdot \ldots \\ &\equiv \prod_{e}(1 + SNR_e^{-1}) \end{aligned} \tag{11}$$

where for each impairing effect $e = \{a, r1, r2, ...\}$ we defined the associated end-to-end inverse gain droop as

$$1 + SNR_e^{-1} \triangleq \prod_{k=1}^{N_s}\left(1 + SNR_{1ek}^{-1}\right). \tag{12}$$

Eq. (11) corresponds to a rearrangement of the blocks in the line where we lump together all similar effects.

A. Onion Peeling

The relation (11) allows the experimentalist to "peel-off" the individual effects from the measured inverse droop $(1 + SNR^{-1})$. We call this procedure "*onion peeling*".

One first removes the ASE contribution, whose $SNR_{1a} = \frac{P_o}{\delta P_a A} = \chi_a^{-1} - 1$ is easily measurable, thus giving us an estimate of $(1 + SNR_a^{-1})$. Then one removes the NLI contribution by computing $SNR_{1NLI} = \frac{P_c}{\alpha_{NL} P_c^3}$, where $P_c = P_o/(N_m N_c)$ is the launched power per channel and $\alpha_{NL}(N_s)$ is the average per-span nonlinear coefficient of the N_s-span link [29, Appendix B], which we can estimate, e.g., from the appropriate GN/EGN model [38], [39]. We thus have an estimate of $(1 + SNR_{NLI}^{-1})$. Then the leftover contribution

$$1 + SNR_r^{-1} \triangleq \frac{1 + SNR^{-1}}{(1 + SNR_a^{-1})(1 + SNR_{NLI}^{-1})} \tag{13}$$

can be analyzed to see, e.g., if it fits a crosstalk/GAWBS model, whose crosstalk coefficient γ_x can be estimated from the following relation (ℓ is the known span length):

$$\gamma_x \ell \equiv SNR_{1r}^{-1} = (1 + SNR_r^{-1})^{1/N_s} - 1 \tag{14}$$

when this estimated quantity is power independent. Estimations at every peeling layer must be accurate, or else a left-over estimation error will be present that might mask the leftover SNR_r (13). Onion peeling was used for instance in [22], [23], [32] (and likely in [21]) to estimate the GAWBS induced penalty and the GAWBS coefficient when operating at very low SNR. More discussion on onion peeling can be found in [26].

IV. GD extension to any amplifier fill-in

Assuming that only signal-carrying modes are amplified, the amplifier fill-in factor is known as bandwidth occupancy [26] and is defined as $\eta_A \triangleq N_c/N_a \leq 1$, where $B_a = N_a B_c$ is the amplifier bandwidth, spanning N_a channel slots of bandwidth B_c. When this factor is not unity, the per-channel RX SNR is:

$$SNR = P_s(N_s)/(\eta_A P_a(N_s) + P_r(N_s)) \tag{15}$$

since now only the in-band ASE $\eta_A P_a$ matters, and SNR does not coincide anymore with the GD-SNR (8). We now need an explicit evaluation of both ASE power $P_a(N_s)$ and rearrangement power $P_r(N_s)$. The detailed derivation of the SNR, called the COP-GD formula, is provided in [29]. The derivation is involved because the span-k rearrangement perturbation $\delta P_{r,k}$ now depends on the total in-band power at the end of span $k-1$, which decreases down the line. We next derive a novel, simple approximation to the exact model, based on the use of a span-independent effective total in-band power. The resulting modified COP-GD formula is much simpler than the rigorous COP-GD [29, eq. (23)], but numerically coincident with it.

A. Simplified COP-GD formula

We tackle here the homogeneous link case for simplicity, while the inhomogeneous case can be treated as in [29]. From the block diagram in Fig. 2 and assuming the perturbation δP_r and thus χ_r are span independent, we get the following update equations for ASE and rearrangement powers out of span k [29, eq. (35)]:

$$P_a(k) = (P_a(k-1) + \delta P_a A \chi_r^{-1})\chi \tag{16}$$

$$P_r(k) = (P_r(k-1) + \delta P_r)\chi \tag{17}$$

whose solution at zero starting conditions after n spans is

$$P_a(n) = P_o(1-\chi_a)\frac{1-\chi^n}{1-\chi} \tag{18}$$

$$P_r(n) = \delta P_r \chi \frac{1-\chi^n}{1-\chi} \tag{19}$$

where, from (3),(4) we have $\chi_a^{-1} = 1 + \frac{\delta P_a A}{P_o}$, and thus we replaced $\delta P_a A \chi_a$ with $P_o(1-\chi_a)$ in (18).

Now, the "effective" power that generates the rearrangement perturbation at span n is saturation power minus out of band power at span $n-1$: $P_o - (1-\eta_A)P_a(n-1)$. If, for the sole computation of such effective power, we upper-bound

$$P_a(n) \le P_o(1-\chi_a^n) \tag{20}$$

(which amounts to pretending that ASE in (18) is drooped by χ_a instead of the true $\chi = \chi_a\chi_r$, a quite reasonable approximation for ASE power, hence we expect the bound to be tight), then the effective total power is $P_o(1-(1-\eta_A)(1-\chi_a^{n-1}))$. Hence the effective *per-channel* power generating perturbation at span n is lower-bounded by [1]

$$P_e(n) \ge P_c(1-(1-\eta_A)(1-\chi_a^{n-1})) \tag{21}$$

where $P_c = P_o/(N_m N_c)$ is the per-channel launch power, and equality holds at $\eta_A = 1$ since P_e cannot be larger than P_c. The span-independent effective power is defined as the average of the (tight) lower-bound (21) over $n \in \{1,..,N_s\}$:

$$\overline{P}_e \triangleq P_c\left[1-(1-\eta_A)\left(1-\frac{1-\chi_a^{N_s}}{N_s(1-\chi_a)}\right)\right]. \tag{22}$$

Finally, the XT/GAWBS and NLI perturbations are computed as

$$\delta P_{XT} = \gamma_x \ell \overline{P}_e \tag{23}$$

$$\delta P_{NLI} = \alpha_{NL}\overline{P}_e^3 \tag{24}$$

where: if XT is the crosstalk (dB/km), then the crosstalk coefficient is $\gamma_x \triangleq 10^{XT/10}$(1/km), with ℓ (km) the span length; and α_{NL} is the average per-span nonlinear coefficient of the N_s-span link [29, Appendix B].

Using now (18),(19) in (15), after some algebra (Appendix 1) we get the simplified COP-GD formula as

$$SNR = \frac{1}{\left[\eta_A + (1-\eta_A)\frac{\chi_r^{-1}-1}{\chi^{-1}-1}\right](\chi^{-N_s}-1)} \tag{25}$$

where $\chi = \chi_a\chi_r$, $\chi_a^{-1} = 1 + \frac{\delta P_a A}{P_o}$, and $\chi_r^{-1} = 1 + \frac{\delta P_{XT}+\delta P_{NLI}}{P_c}$. We verified that Eq. (25) numerically coincides to several decimal digits with the exact COP-GD [29, eq. (23)] in all the cases tested in [29], but is much easier to evaluate.

Using the same average effective power trick, Appendix 2 shows how to simplify also the CG-GD formula [29, eq. (29),(23)] with numerically coinciding results, reproducing, e.g., the CG-GDF curve in [29, Fig.10]. So we now also have a simple closed-form SNR expression for CG links with ASE+NLI that improves on the low-SNR heuristic model in [40].

Unfortunately Eq. (25) does not satisfy the GD cascading rule (9). However Appendix 1 shows that the GD cascading rule still applies if we use instead the following tight upper-bound to the COP-GD SNR

$$SNR_{UB} = \frac{1}{\chi_r^{-N_s}\left(1+\eta_A(\chi_a^{-N_s}-1)\right)-1} \tag{26}$$

which is exact at $\eta_A = 1$ for all N_s, and at $N_s = 1$ for all η_A. Eq. (26) amounts to isolate the in-band contribution of ASE induced droop, then to use the GD formula in the channel band. The approximation error SNR_{UB}/SNR is worst when N_s is large and η_A is small, at fixed SNR_{1a} (4) and SNR_{1r} (7). The larger the SNR_1's, the smaller the error. SNR_{1a} is more critical than SNR_{1r} (i.e., if one of the two must be small, better be SNR_{r1}). The error in dB decreases linearly with N_s. For example, at $SNR_{1a} = 25$dB (on the small side, cfr. Fig. 1) and $SNR_{1r} = 30$dB (typical), we get an error 0.36dB at $\eta_A = 0.5$ and $N_s = 300$ spans. When both SNR_1 are 30dB the error goes down to 0.22dB at $(\eta_A = 0.5, N_s = 300)$ and to 0.11dB at $(\eta_A = 0.5, N_s = 150)$. So overall the error is quite small, and eq. (26) can be taken as a safe cascadable GD SNR formula at all practical amplifier fill-in factors $\eta_A \ge 0.5$.

[1] In [29] we defined $\beta \triangleq \delta P_a A/N_a/N_m$ as the per-channel generated output ASE power when the gain equals A, which by (3) is $\beta = P_c\eta_A\chi_a/(1-\chi_a)$. Hence (21) becomes: $P_e(n) \ge P_c - \beta\chi_a(\frac{1}{\eta_A}-1)\frac{1-\chi_a^{n-1}}{1-\chi_a}$, which is eq. (25) in [29], except that $\beta\chi_a$ here was erroneously replaced by β there, without numerical consequences since $\chi_a \cong 1$.

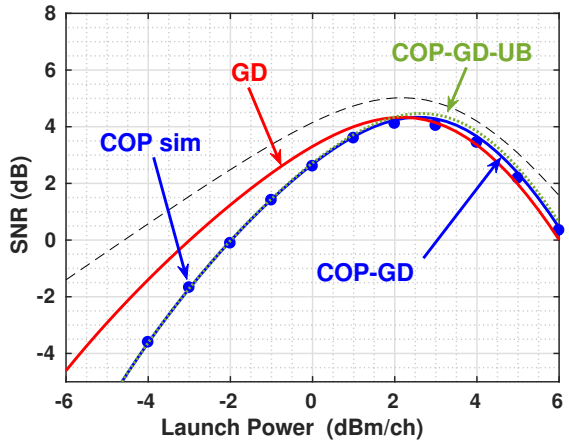

Figure 4. SNR versus launch power per channel P_c in 40x120km NZDSF link of Case C in [29], at COP saturation power $P_o = N_c P_c$. Main data: N_c =15 PDM-QPSK channels, B_c =49GHz, span loss $A = 26.4$dB, noise figure $F = 5$dB. ASE filtered on WDM bandwidth, channel spacing $\Delta f = 100$GHz, yielding $\eta_A = 0.49$. We show: the basic GD at $\eta_A = 1$, eq. (8); the COP-GD eq. (25); and the COP-GD-UB eq. (26). Symbols: SSFM simulations. Dashed line: standard GSNR for CG link, where amplifiers have constant gain $G = A$.

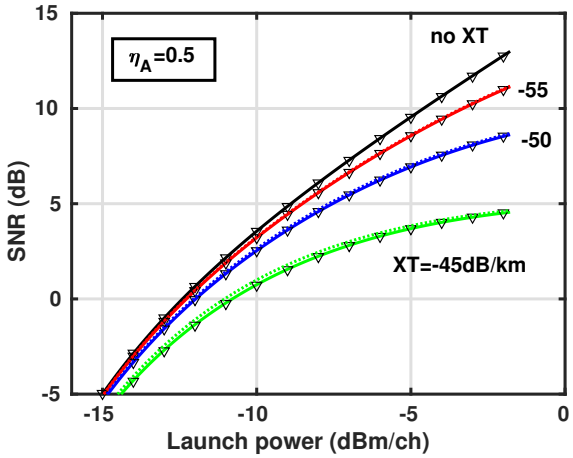

Figure 5. SNR versus launch power per channel P_c in 133x60km EX2000 link in [31], at several crosstalk levels and COP saturation power $P_o = N_c P_c$. Main data: $N_c = 60$ channels, $B_c = 70$GHz, span loss $A = 9.24$dB, noise figure $F = 5$dB. ASE filtered on WDM bandwidth, channel spacing $\Delta f = 140$GHz, yielding $\eta_A = 0.5$. We show: (solid) the COP-GD eq. (25); and (dotted) the COP-GD-UB eq. (26). Symbols: SSFM simulations.

B. Numerical examples

A first example with a single-mode link with ASE and NLI only is provided in Fig. 4. The figure shows the RX SNR vs. launch power per channel P_c in a $N_s = 40$ span non-zero-dispersion shifted (NZDSF) single-mode link with span length ℓ=120km with N_c =15 polarization division multiplexed - quadrature phase shift keying (PDM-QPSK) channels at B_c =49GHz (Case C in [29]). ASE is filtered on the WDM bandwidth, and the channel spacing is $\Delta f = 100$GHz, yielding $\eta_A = 0.49$. We show: the basic GD eq. (8) at $\eta_A = 1$; the COP-GD eq. (25); and the COP-GD-UB eq. (26). Symbols: Split-Step Fourier Method (SSFM) simulations (all details in [29]). Dashed line: standard GSNR for CG link, where amplifiers have constant gain $G = A$. We see that the GD formula (8) at $\eta_A = 1$ (same as (25) at $\eta_A = 1$) over-estimates the SNR at low powers (the regime of interest in submarine SDM) and under-estimates the SNR at high-power because for NLI evaluation it uses P_c instead of the lower effective power $\overline{P}_e$ (22). We note that the "cascadable" COP-GD-UB is almost undistinguishable from the exact COP-GD even at this low bandwidth occupancy. We also report in dashed line the standard GSNR for ASE+NLI, to show how far it is from simulations at these low SNRs.

A second example with a single-mode link with ASE and XT only is provided in Fig. 5. The figure shows the RX SNR vs. launch power per channel P_c in the 133x60km EX2000 link in [31], at several crosstalk levels. The main data are: $N_c = 60$ channels (modulation format is unimportant since here we do not have NLI), $B_c = 70$GHz, span loss $A = 9.24$dB, noise figure $F = 5$dB. ASE is filtered on the WDM bandwidth, with channel spacing $\Delta f = 140$GHz, yielding $\eta_A = 0.5$. We show: (solid) the COP-GD eq. (25); and (dotted) the COP-GD-UB eq. (26). Symbols are SSFM simulations. We see that the COP-GD has an excellent match with simulations, and the COP-GD-UB becomes distinguishable from the COP-GD only at the lowest powers and at the largest XT=-45dB/km.

V. Power efficiency optimization

One key parameter for the optimization of submarine SDM systems is the power efficiency (PE). It may be defined as in Sinkin *et al.* [6]: $PE_S \triangleq C/(N_s P_o)$ where the repeater output optical power P_o equals the total signal launched power. It may also be defined as in Downie et al. [8], [33], [34] as $PE_D \triangleq C/(N_s P_p)$ where P_p is the (electrical) repeater pump power, which is a function of the line feed voltage [7], [12], [35], [36]. We elaborate here on the PE maximization results in [6], [8], [10], [31], [32] and report a few original extensions derived with our GD/COP-GD formulas.

A. Sinkin's power efficiency

When N_s is large (in practice $N_s \gtrsim 30$), by following the derivations in [6], [31], we show in Appendix 3 the following results.

1) any η_A, ASE only: With ASE only at any fill-in η_A, using the COP-GD we have:

$$PE_S \cong \eta_A K \log_2(1 + \Gamma SNR) \ln(1 + (\eta_A SNR)^{-1}) \quad (27)$$

with

$$K \triangleq 2/(h f_0 F A N_s^2). \quad (28)$$

Note that the shape of the PE_S vs. SNR curve is distance independent (for $N_s \gtrsim 30$), with just a "vertical" scaling with N_s due to the K factor. The distance-independent maximum of PE_S occurs exactly at

$$SNR^*(dB) = (\eta_A^{dB} + \Gamma^{dB})/2 \quad (29)$$

with $\eta_A^{dB} \triangleq -10\log_{10}(\eta_A)$ and $\Gamma^{dB} \triangleq -10\log_{10}(\Gamma)$, independently of any other system parameter. At $\eta_A = 1$ this result first appeared in [32], while eq. (29) is new.

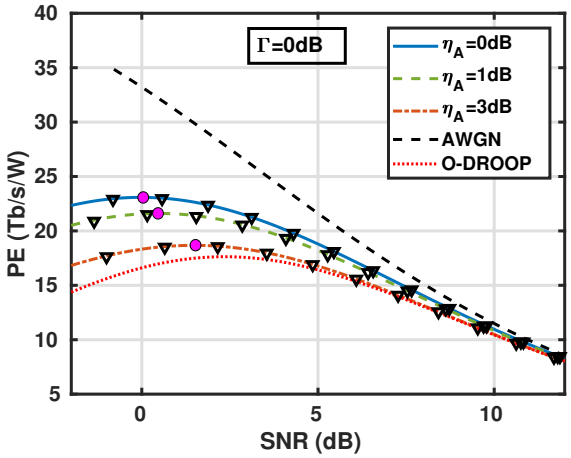

Figure 6. PE_S (Tb/s/W) versus received SNR (dB) [eq. (27) , thick lines] for 8000km EX2000 link [31] at various fill-in factors $\eta_A = [0, 1, 3]$dB. Gap to Shannon Γ=1. Dashed (AWGN) and dotted (O-DROOP) curves are the "AWGN" and "Original Droop" PE curves in [31, Fig. 4b]. Triangles are SSFM simulations. Filled circles are the location of the maxima at the predicted value (29).

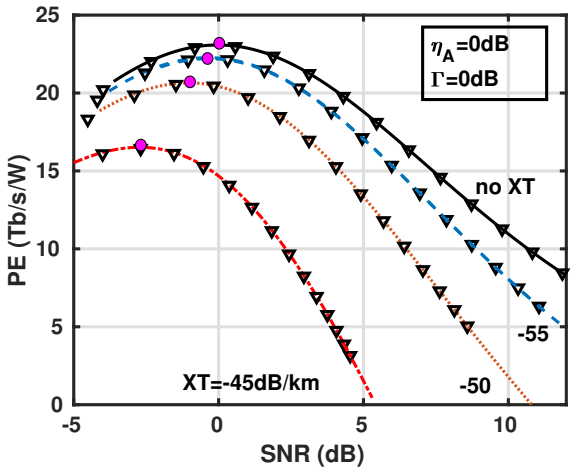

Figure 7. Power efficiency PE_S (Tb/s/W) eq. (30) versus received SNR (dB) for 8000km EX2000 link [31, Fig. 7]. Solid: no XT; Dashed: XT=-55 dB/km; dotted: XT=-50 dB/km; dash-dotted: XT=-45 dB/km. Triangles: SSFM simulations. Circles: PE maxima. Data: $\eta_A = 0$dB, $\Gamma = 0$dB.

Fig. 6 shows in solid line PE_S eq. (27) vs. RX SNR for the same 8000km EX2000 link [31] at various values of η_A. The $\eta_A = 0$dB curve is the same as the "GD model" curve in [31, Fig. 4b]. Also shown are the "AWGN" (dashed) and "Original Droop" (dotted) PE curves in [31, Fig. 4b], which were obtained at full amplifier fill-in $\eta_A = 0$dB by using either the standard cascading SNR formula or Sinkin's drooped SNR [6, eq.(3)], respectively . Triangles are SSFM simulations, which double-check the accuracy of the analytical formula (27). The maximum is confirmed to be exactly at $\eta_A^{dB}/2$ (here $\Gamma^{dB} = 0$), as shown by the filled circles. Sinkin's original droop model would predict an optimum at $SNR^* = 2.36$dB, which is closer to typical experiments [10] than the true optimum at $0 = \Gamma^{dB}$. An explanation of this fact is deferred to the next section. The whole PE_S curve is seen to decrease when decreasing η_A. Note that when SNR is large, the curves for all η_A tend to converge to the $\eta_A = 1$ standard case because ASE saturation is less and less important.

2) at $\eta_A = 1$, ASE+XT: With ASE and XT at $\eta_A = 1$, using the GD SNR, Appendix 3 proves that:

$$PE_S \cong K \log_2(1+\Gamma SNR) \frac{\ln(1+SNR^{-1}) - N_s \gamma_x \ell}{1+\gamma_x \ell} \quad (30)$$

with K as in (28). Now we see that increasing the spans N_s changes also the shape of the PE_S vs. SNR curve, hence there ceases to be a universal optimum SNR^* for all distances. While the maximum without XT is reached at $SNR^* = 1/\sqrt{\Gamma}$, analysis of the derivative with respect to SNR reveals that the more the crosstalk or the span count, the more the optimal SNR^* is reached before $1/\sqrt{\Gamma}$.

Fig. 7 shows (lines) PE_S eq. (30) vs. RX SNR for the same 8000km EX2000 link [31] at various values of XT. Triangles are SSFM simulations, which double-check the accuracy of the analytical formula (30). We see that XT has the effect of lowering PE and its optimum SNR.

B. Downie's power efficiency, ASE only.

Power efficiency may also be defined as in Downie *et al.* [8], [33], [34] as $PE_D = C/(N_s P_p)$ where P_p is the (multi-mode or multi-fiber) repeater pump power.

Assume for simplicity we have only ASE, and that as in [8], [35] the repeater output power is described by a diode-like affine law $P_o = \max(0, \eta(P_p - P_{p0}))$, where P_{p0} is a "transparency" pump value below which the repeater is off, and η is the electrical-to-optical power conversion efficiency. Since SNR_1 depends on P_o as per (4), then an affine law is induced on SNR_1 as

$$SNR_1 = \max(0, SNR_{1o} - \Delta SNR_1) \quad (31)$$

with $SNR_{1o} = \frac{\eta P_p}{\delta P_a A}$ our "free variable", and $\Delta SNR_1 = \frac{\eta P_{p0}}{\delta P_a A}$ a "wasted SNR_1". Hence we can scan the free variable SNR_{1o} at fixed ΔSNR_1, and obtain: 1) the induced $SNR_1 = SNR_{1o} - \Delta SNR_1$; 2) the received $SNR = ((1 + SNR_1^{-1})^{N_s} - 1)^{-1}$; and 3) the capacity $C = 2B_c N_c \log_2(1 + \Gamma SNR)$. Thus we have

$$PE_D \propto f = \ln(1+\Gamma SNR)/SNR_{1o} \quad (32)$$

and we plot it versus SNR to find its maximizing SNR^*. Except for an irrelevant vertical scaling, the PE_D vs. SNR curve just depends on the three parameters ΔSNR_1, Γ, and N_s, which summarize all remaining system parameters, such as fiber type, span loss, span length, etc.

Fig. 8 shows (solid lines) the optimum SNR^* versus number of spans N_s at several values of ΔSNR_1, for $\Gamma = 0$dB (same as [32, Fig. 2(right)]). We note the important dependence of the optimal RX SNR on the span number N_s when the "wasted SNR_1" becomes large. When $\Delta SNR_1 = 0$ we retrieve the optima of Sinkin's PE_S since now it is proportional to PE_D. All curves converge to the $\Delta SNR_1 = 0$ ideal case as $N_s \to \infty$, but at greatly different speed depending on ΔSNR_1. When the gap to capacity is increased to Γ^{dB}, in practice all curves almost shift up by $\Gamma^{dB}/2$. When N_s is

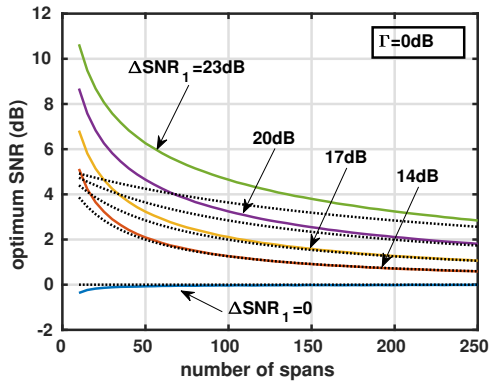

Figure 8. Optimum received SNR^* that maximizes power efficiency $PE_D = C/P_p$ plotted versus number of spans (i.e., repeaters) N_s, at several values of ΔSNR_1. Gap $\Gamma = 0$dB; Dotted lines: SNR^* perturbative approximation, eq. (33).

large (in practice $N_s \gtrsim 30$) , Appendix 4 derives the following perturbative approximation to SNR^* :

$$SNR^* \cong \frac{1}{\sqrt{\Gamma}} \left[1 + \frac{r}{2\left[\frac{\sqrt{\Gamma}}{1+\sqrt{\Gamma}} \left(\frac{1}{\ln(1+\sqrt{\Gamma})} + 1 \right) - 1 \right]} \right] \quad (33)$$

where

$$r = \frac{1}{\frac{N_s}{\ln(1+\sqrt{\Gamma})\Delta SNR_1} + 1}. \quad (34)$$

Approximation (33) is plotted in Fig. 8 in dotted lines and is a very good lower-bound to the true SNR^* whenever $r \leq 0.25$, i.e., at

$$N_s \geq 3 \ln(1+\sqrt{\Gamma}) \Delta SNR_1 \quad (35)$$

which ensures an error in SNR^* less than 0.1dB. From observation of the curves in Fig. 8 we now understand that the experimentally observed optimal SNR values around 2.36dB [10] as in Sinkin's original droop model are indeed also found by the optimization of Downie's PE_D when using the GD model.

VI. Summary and Conclusions

We reviewed two recently published almost-identical GD models [29], [31]. We reviewed the extension of the GD formula (the COP-GD formula [29]) to the case where the WDM signals do not entirely occupy the COP amplifier bandwidth. We finally showed the use of the GD formula in optimizing the power efficiency in SDM submarine links.

New results in this paper are: 1) a simplified GD formula for COP links at non-full bandwidth fill-in, eq. (25) and the corresponding simplified SNR formula for CG links, eqs. (41),(42); 2) an approximate cascading formula for COP-GD, eq. (40), and the corresponding COP-GD SNR upper-bound, eq. (26); 3) the large-span expression of Sinkin's power efficiency PE_S at full bandwidth fill-in with ASE+XT, eq. (27), and at lower than 1 fill-in and ASE only, eq. (30); 4) the optimum SNR maximizing $PE_S = C/(N_s P_o)$ at lower than 1 fill-in with ASE only, eq. (29); 5) the perturbation-approximation (33) of the optimum SNR that maximizes Downie's $PE_D = C/(N_s P_p)$ when an affine model of P_o versus P_p holds.

Please note that, as seen in Fig. 8, the power efficiency optimization leads to per-channel SNRs of a few dB, in the so-called deeply linear regime [21], which implies submarine systems with a very large number of SDM paths and thus of amplifiers and transponders. One should be aware that techno-economic analyses that also account for hardware cost, based on today's technology, hint at using fewer SDM paths than the power-efficiency optimal number and thus larger SNRs, just ~1.5-2 dB below the maximum nonlinear SNR [7], [10]. If significant cost reductions by SDM integration will be achieved in the future, then the cost-optimal number of SDM paths per cable will increase [7, Fig. 10] and thus SNRs will be lowered more and more towards the deeply linear regime.

We close with a word of caution about two known limitations of the GD model:

1) In classical CG links where nonlinear interference is important we know that if we have for example a type 1 fiber in the first half of the link, followed by a type 2 fiber in the rest of the link (we call this a T1-T2 line), then the end-to-end performance in presence of NLI is different from that of the T2-T1 line. However, the intrinsic commutativity of the GD model blocks would incorrectly imply they are equivalent for COP links. To make the GD model work correctly and yield the same SNR value as the GSNR in high-SNR CG links, we use the following trick, discussed at length in [29, App. B]. We first compute the end-to-end NLI coefficient a_{NL} over the link N_s spans, and then use the average $\alpha_{NL} = a_{NL}/N_s$ as the NLI coefficient within each span. This way, the GD model yields the correct SNR values [29, App. B, Fig. 11]. So, the commutativity of the GD model blocks for NLI is only an apparent artifact. Hence one should not try and infer from the GD model the structure of a possible NLI compensator. Compensators do need also information on the field phase, which is not retained by the GD model.

2) The GD model is intrinsically scalar and does not discriminate the two polarizations of each spatial mode, it just considers their lumped power. Therefore any polarization effects, such as polarization mode dispersion and polarization dependent loss, cannot be captured by the GD model, although they are mostly suppressed by the coherent receiver.

Acknowledgments

A. Bononi and P. Serena acknowledge support from Ministero dell'Istruzione, dell'Università e della Ricerca (FIRST, PRIN 2017).

Appendix 1: The simplified COP-GD

We show here how to derive the simplified COP-GD equation (25). Substituting (18),(19) and also $P_s(N_s) = P_o \chi^{N_s}$ in

(15) we get:

$$SNR = \frac{P_o\chi^{N_s}}{[\eta_A P_o(1-\chi_a)+\delta P_r\chi]\frac{1-\chi^{N_s}}{1-\chi}} = \frac{\chi^{N_s}}{\left[\eta_A(1-\chi_a)+(\chi_r^{-1}-1)\chi\right]\frac{1-\chi^{N_s}}{1-\chi}} = \frac{1}{\left[\eta_A-\frac{\eta_A(1-\chi)}{1-\chi}+\frac{\eta_A(1-\chi_a)}{1-\chi}+\frac{(\chi_r^{-1}-1)\chi}{1-\chi}\right](\chi^{-N_s}-1)}$$

where in the second line we used $\delta P_r = P_o(\chi_r^{-1}-1)$, and in the third line we added and subtracted η_A. So

$$SNR = \frac{1}{\left[\eta_A-\frac{\eta_A(-\chi+\chi_a)}{1-\chi}\chi^{-1}\chi+\frac{(\chi_r^{-1}-1)\chi}{1-\chi}\right](\chi^{-N_s}-1)} = \frac{1}{\left[\eta_A-\frac{\eta_A(\chi_r^{-1}-1)}{1-\chi}\chi+\frac{(\chi_r^{-1}-1)\chi}{1-\chi}\right](\chi^{-N_s}-1)}$$

which leads to eq. (25). This "exact" expression does not yield a cascading form. However,

$$\begin{aligned} 1+SNR^{-1} &= \frac{P_s(N_s)+\eta_A P_a(N_s)+P_r(N_s)}{P_s(N_s)} \\ &= \frac{P_o-(1-\eta_A)P_a(N_s)}{P_s(N_s)} \\ &\geq \frac{P_o-P_o(1-\eta_A)(1-\chi_a^{N_s})}{P_o\chi_a^{N_s}\chi_r^{N_s}} \\ &= \chi_r^{-N_s}\left(1+\eta_A(\chi_a^{-N_s}-1)\right) \end{aligned} \tag{36}$$

where in the third line we used the upper-bound (20). Now,

$$\chi_r^{-N_s} = 1+SNR_r^{-1} \tag{37}$$

is the RX SNR formula for the r-noise-only case. Also,

$$\chi_a^{-N_s}-1 = SNR_{GD,a}^{-1} \tag{38}$$

is the GD-SNR formula *with only ASE*, namely $SNR_{GD,a} \triangleq \frac{P_s(N_s)}{P_a(N_s)}$. If we consider the per-channel RX SNR with only ASE: $SNR_a \triangleq \frac{P_s(N_s)}{\eta_A P_a(N_s)}$, then we see that $SNR_a = SNR_{GD,a}/\eta_A$, hence from the GD-SNR $\eta_A(\chi_a^{-N_s}-1) = SNR_a^{-1}$, and therefore

$$\left(1+\eta_A(\chi_a^{-N_s}-1)\right) = 1+SNR_a^{-1}. \tag{39}$$

Thus finally using (37),(39) in (36) we get the approximate cascading formula for the $\eta_A < 1$ case:

$$1+SNR^{-1} \geq \left(1+SNR_a^{-1}\right)\left(1+SNR_r^{-1}\right) \tag{40}$$

which leads to the upper bound (26).

APPENDIX 2: THE SIMPLIFIED CG-GD

Using the same idea as in Appendix 1, we can also simplify the CG case with NLI induced saturation in the highly nonlinear regime. In [29] we claim that again [29, eq. (23)] applies with the substitutions: $\eta_A \to 1$; $(\chi_a^{-1}-1) \to \beta/P_c$; $\chi_k \to \chi_{rk}$; $\chi_{rk}^{-1} \to 1+\alpha_{NL}P_e(k)^3/P$, where $P_e(k) = P_c+(k-1)\beta$, where $\beta \triangleq \delta P_a A/(N_a N_m) = hf_0 FAB_c$. So using now the link-averaged effective power

$$\overline{P}_e = P_c+\beta\frac{1}{N_s}\sum_{k=1}^{N_s}(k-1) = P_c+\frac{\beta(N_s-1)}{2}$$

in place of $P_e(k)$ we get from [29, eq. (23)]:

$$SNR_{CG-GD} = \frac{1}{[1+\frac{\beta}{P_c}\frac{\chi_r^{-1}}{\chi_r^{-1}-1}](\chi_r^{-N_s}-1)} \tag{41}$$

with

$$\chi_r^{-1} = 1+\alpha_{NL}\frac{\overline{P}_e^3}{P_c} = 1+\alpha_{NL}P_c^2\left(1+\frac{\beta(N_s-1)}{2P_c}\right). \tag{42}$$

We verified that this simplified CG-GD formula for the cases A, B, C in [29] numerically coincides with the rigorous CG-GD formula in [29] up to several decimal digits.

APPENDIX 3: SINKIN'S POWER EFFICIENCY

Sinkin *et al.* [6] defined the power efficiency as the ratio of capacity to total power out of all repeaters in the line: $PE_S = C/(N_s P_o)$, with C as in (1). We wish to study PE_S versus the per-tributary RX SNR and find the optimal SNR maximizing PE_S. We will restrict the analysis to the "deeply linear" regime [21] where NLI can be neglected.

A. General fill-in η_A, ASE only

The COP-GD formula (25) with ASE only ($\chi_r = 1$) gives: $SNR = (\eta_A(\chi_a^{-N_s}-1))^{-1}$, hence using (3)

$$(1+(\eta_A SNR)^{-1})^{1/N_s} = \chi_a^{-1} \equiv 1+\frac{\delta P_a A}{P_o}$$

thus

$$N_s P_o = \frac{N_s\delta P_a A}{(1+(\eta_A SNR)^{-1})^{1/N_s}-1} \tag{43}$$

hence using (2) in (43), and capacity as (1) we get for power efficiency:

$$PE_S = \eta_A K\log_2(1+\Gamma\,SNR)N_s((1+(\eta_A SNR)^{-1})^{\frac{1}{N_s}}-1) \tag{44}$$

where

$$K(N_s) \triangleq \frac{2}{hf_0\,F\,A\,N_s^2}. \tag{45}$$

Since for any a it is $\lim_{N\to\infty} N((1+a)^{1/N}-1) = \ln(1+a)$, then for large N_s we have

$$PE_s \to \eta_A K\log_2(1+\Gamma\,SNR)\ln(1+(\eta_A SNR)^{-1}) \tag{46}$$

where convergence for any $\eta_A \geq 0.5$ and $SNR > 0$dB is practically achieved for $N_s \gtrsim 30$.

Call x the SNR. To find the optimal SNR we set to zero the derivative of $PE_S \propto f(x) = \ln(1+\Gamma x)\ln(1+(\eta_A x)^{-1})$ namely:

$$f'(x) = \Gamma\frac{\ln(1+(\eta_A x)^{-1})}{1+\Gamma x}-\frac{\ln(1+\Gamma x)}{\eta_A x^2(1+(\eta_A x)^{-1})} = 0 \tag{47}$$

whose solution by inspection is when $(\eta_A x)^{-1} = \Gamma x$, i.e., when $x = 1/\sqrt{\Gamma\eta_A}$.

B. $\eta_A = 1$ and ASE+XT

At $\eta_A = 1$ with ASE and XT we use the GD cascading rule (9) to get

$$1 + SNR^{-1} = \left(1 + \frac{\delta P_a A}{P_o}\right)^{N_s} (1 + \gamma_x \ell)^{N_s}$$

hence

$$N_s P_o = \frac{N_s \delta P_a A}{\frac{(1+SNR^{-1})^{1/N_s}}{1+\gamma_x \ell} - 1}. \tag{48}$$

Using (2) in (48), and capacity as (1) we get for power efficiency:

$$PE_S = K \log_2(1 + \Gamma\, SNR) N_s \left(\frac{(1 + SNR^{-1})^{1/N_s}}{1 + \gamma_x \ell} - 1\right) \tag{49}$$

with $K(N_s)$ as in (45). Again for large N_s we get

$$PE_S \to K(N_s) \log_2(1 + \Gamma\, SNR) \frac{\ln(1 + SNR^{-1}) - N_s \gamma_x \ell}{1 + \gamma_x \ell}. \tag{50}$$

We note that PE_S with XT becomes non-physical (negative values) at "large" SNR, when $\ln(1 + SNR^{-1}) < N_s \gamma_x \ell$. or equivalently in the non-asymptotic formula when $\left(1 + SNR^{-1}\right)^{1/N_s} \leq 1 + \gamma_x \ell$, which implies $SNR \geq ((1 + \gamma_x \ell)^{N_s} - 1)^{-1}$. This is clear, since the SNR cannot be higher than that due only to XT. That's the maximum possible SNR in presence of XT.

Appendix 4: Proof of eqs. (33)-(34)

Let $SNR = x$. We wish to get the maximum of $PE_D \propto f(x) = \ln(1 + \Gamma x)/SNR_{1o}$. We need to zero out the following derivative $f'(x) \equiv \frac{\partial f}{\partial x} = \frac{\partial f}{\partial SNR_1} \frac{1}{\frac{\partial x}{\partial SNR_1}}$, where we compute

$$\begin{aligned} \frac{\partial x}{\partial SNR_1} &= \frac{\partial \left((1 + SNR_1^{-1})^{N_s} - 1\right)^{-1}}{\partial SNR_1} \\ &= M \frac{x}{SNR_1} \frac{1 + x}{1 + SNR_1} \end{aligned} \tag{51}$$

and

$$\frac{\partial f}{\partial SNR_1} = \frac{1}{SNR_{1o}} \left[\frac{\Gamma}{1 + \Gamma x} \frac{\partial x}{\partial SNR_1} - \frac{\ln(1 + \Gamma x)}{SNR_{1o}}\right] \tag{52}$$

so that

$$SNR_{1o} f'(x) = \frac{\Gamma}{1 + \Gamma x} - \frac{\ln(1 + \Gamma x)}{SNR_{1o}} \frac{SNR_1}{N_s \cdot x} \frac{1 + SNR_1}{1 + x}.$$

Now we notice that $N_s SNR_1^{-1} = N_s((1+x^{-1})^{1/N_s} - 1) \to \ln(1+x^{-1})$ as $N_s \to \infty$, with convergence already at $N_s \gtrsim 30$ for any meaningful SNR x. Thus at "large" N_s we zero out the derivative and get the equation

$$\frac{\Gamma}{1 + \Gamma x} - \frac{\ln(1 + \Gamma x)}{\ln(1 + x^{-1})} \frac{1}{x^2(1 + x^{-1})}(1 - r) = 0 \tag{53}$$

where we set $1 - r \triangleq \frac{1+SNR_1}{SNR_{1o}}$ so that $r \sim \frac{\Delta SNR_1}{SNR_{1o}} \ll 1$.

Now, when $r = 0$, eq. (53) equals eq. (47) at $\eta_A = 1$, whose solution is $x_o = 1/\sqrt{\Gamma}$. So the strategy is to assume a perturbed solution $x = x_o + \delta x$, substitute into (53), discard all terms of order smaller than δx and relate the solving perturbation δx to r. To that aim, we note that by the same above limit we get

$$r \to \frac{1}{\frac{N_s}{\ln(1+x_o^{-1})\Delta SNR_1} + 1} \tag{54}$$

where we replaced x with x_o. Also, for $x = x_o + \delta x$ we get to first order in δx :

$$1 + \Gamma x = (1 + \sqrt{\Gamma})(1 + \frac{\Gamma \delta x}{1 + \sqrt{\Gamma}}) \tag{55}$$

$$1 + x^{-1} \cong (1 + \sqrt{\Gamma})(1 - \frac{\Gamma \delta x}{1 + \sqrt{\Gamma}}) \tag{56}$$

$$x^2 \cong \frac{1}{\Gamma}(1 + 2\sqrt{\Gamma}\delta x) \tag{57}$$

$$\ln(1 + \Gamma x) \cong \ln(1 + \sqrt{\Gamma}) \left[1 + \frac{\Gamma}{1 + \sqrt{\Gamma}} \frac{\delta x}{\ln(1 + \sqrt{\Gamma})}\right] \tag{58}$$

$$\ln(1 + x^{-1}) = \ln(1 + \sqrt{\Gamma}) \left[1 - \frac{\Gamma}{1 + \sqrt{\Gamma}} \frac{\delta x}{\ln(1 + \sqrt{\Gamma})}\right]. \tag{59}$$

Now substitute $x = x_o + \delta x$ into (53) and use (55)-(59), cancel common terms, keep constant terms and terms in δx, and throw off everything else, obtaining:

$$\delta x = \frac{r}{2\sqrt{\Gamma}\left[\frac{\sqrt{\Gamma}}{1+\sqrt{\Gamma}}\left(\frac{1}{\ln(1+\sqrt{\Gamma})} + 1\right) - 1\right]}$$

so that the perturbed optimum is $SNR^* = x_o + \delta x$, with r given in (54).

References

[1] N. S. Bergano, "Undersea communication systems," in I. Kaminow and T. Li (Ed.), *Optical fiber telecommunications IVB*. Ch. 4. San Diego, CA, USA: Academic Press, 2002.

[2] T. Frishch and S. Desbruslais, "Electical power, a potential limit to cable capacity," in *Proc. SubOptic*, Paris, France, 2013, Paper TUIC-04.

[3] C. R. Giles and E. Desurvire, "Propagation of signal and noise in concatenated Erbium-doped fiber optical amplifiers," *J. Lightw. Technol.*, vol. 9, no. 2, pp. 147-154, Feb. 1991.

[4] A. R. Chraplyvy, "The coming capacity crunch," in *Proc. Eur. Conf. Opt. Commun.*, Vienna, Austria, 2009, Plenary talk.

[5] O. V. Sinkin, *et al.*, "Maximum optical power efficiency in SDM-based optical communication systems," *IEEE Photon. Technol. Lett.*, vol. 29, no. 13, pp. 1075-1077, May 2017.

[6] O. V. Sinkin *et al.*, "SDM for power-efficient undersea transmission," *J. Lightw. Technol.*, vol. 36, pp. 361-371, Jan. 2018.

[7] R. Dar *et al.*, "Cost-optimized submarine cables using massive spatial parallelism," *J. Lightw. Technol.*, vol. 36, pp. 3855-3865, Sep. 2018.

[8] J. K. Perin, *et al.*, "Importance of amplifier physics in maximizing the capacity of submarine links," *J. Lightw. Technol.,* vol. 37, pp. 2076-2085, May 2019.

[9] P. Pecci *et al.*, "Pump farming as enabling factor to increase subsea cable capacity," in *Proc. Suboptic*, New Orleans (LA), USA, 2019, Paper OP-14.4.

[10] M. A. Bolshtyansky *et al.*, "Single-mode fiber SDM submarine systems," *J. Lightw. Technol.*, vol. 38, no. 6, pp. 1296-1304, Mar. 2020.

[11] J. D. Downie, "Maximum capacities in submarine cables with fixed power constraints for C-band, C+L band, and multicore fiber systems," *J. Lightw. Technol.*, vol. 36, no. 18, pp. 4025-4032, Sep. 2018.

[12] J. D. Downie, X. Liang and S. Makovejs, "Assessing capacity and cost/capacity of 4-Core multicore fibers against single core fibers in submarine cable systems," *J. Lightw. Technol.*, vol. 38, no. 11, pp. 3015-3022, Jun. 2020.

[13] J. D. Downie, X. Liang, and S. Makovejs, "Examining the case for multicore fibers in submarine cable systems based on fiber count limits," *IEEE J. Sel. Topics Quantum Electron.*, vol. 26, no. 4, pp. 1–9, 2020.

[14] P. J. Winzer and G. J. Foschini, "MIMO capacities and outage probabilities in spatially multiplexed optical transport systems," *Opt. Express*, vol. 19, no. 17, pp. 16680-3599, Aug. 2011.

[15] P. J. Winzer, "Energy-efficient optical transport capacity scaling through spatial multiplexing," *IEEE Photon. Technol. Lett.*, vol. 23, no. 13, pp. 851-853, Jul. 2011.

[16] R.-J. Essiambre and R. Tkach, "Capacity trends and limits of optical communication networks," in *Proc. IEEE*, vol. 100, no. 5, pp. 1035–1055, May 2012.

[17] E. F. Mateo and F. Yaman, "Nonlinearity compensation in modern submarine networks," in *Proc. OptoElectron. Commun. Conf. and Int. Conf. Photon. Switch. Comp.*, Fukuoka, Japan, 2019, pp. 1-3.

[18] J. M. Gené and P. J. Winzer "A universal specification for multicore fiber crosstalk," *IEEE Photon. Technol. Lett.*, vol 31, n. 9, pp. 673-676, 2019.

[19] M. A. Bolshtyansky *et al.*, " Impact of spontaneous guided acoustic-wave Brillouin scattering on long-haul transmission ," in *Proc. Opt. Fiber Commun. Conf.,* San Diego (CA), USA, 2018, Paper M4B.3.

[20] M. Nakazawa *et al.*, "Observation of guided acoustic-wave Brillouin scattering noise and its compensation in digital coherent optical fiber transmission," *Opt. Express* vol. 26, pp. 9165–9181, 2018.

[21] V. Ivanov, J. Downie, and S. Makovejs, "Modeling of guided acoustic waveguide Brillouin scattering impact in long-haul fiber optic transmission systems," in *Proc. Eur. Conf. Opt. Commun.*, Brussels, Belgium, 2020, Paper Tu2E-6.

[22] J.-C. Antona *et al.*, Performance of open cable: from modeling to wide scale experimental assessment," in *Proc. SubOptic,* New Orleans (LA), USA, 2019, Paper OP-7.1.

[23] J. C. Antona, A. C. Meseguer, S. Dupont, R. Garuz, P. Plantady, A. Calsat, and V. Letellier, "Analysis of 34 to 101GBaud submarine transmissions and performance prediction models," in *Proc. Opt. Fiber Commun. Conf.,* San Diego (CA), USA, 2020, Paper T4I.3.

[24] V. Kamalov *et al.,* "The subsea fiber as a Shannon channel," in *Proc. SubOptic*, New Orleans (LA), USA, 2019, Paper OP-12.2.

[25] E. Rivera Hartling *et al.*, "Subsea open cables: A practical perspective on the guidelines and gotchas," in *Proc. SubOptic*, New Orleans (LA), USA, 2019.

[26] E. Rivera Hartling *et al.*, "Design, Acceptance and Capacity of Subsea Open Cables," *J. Lightw. Technol.* vol. 39, pp. 742-756, 2021.

[27] J. Antona, A. C. Meseguer and V. Letellier, "Transmission systems with constant output power amplifiers at low SNR values: a generalized droop model," in *Proc. Opt. Fiber Commun. Conf.,* San Diego (CA), USA, 2019, Paper M1J.6.

[28] A. Bononi, J.-C. Antona, A. Carbo Meseguer, and P. Serena, "A model for the generalized droop formula" in *Proc. Eur. Conf. Opt. Commun.*, Dublin, Ireland, 2019, Paper W.1.D.5.

[29] A. Bononi, J.-C. Antona, M. Lonardi, A. Carbo-Meseguer, and P. Serena, "The generalized droop formula for low signal to noise ratio optical links," *J. Lightw. Technol.*, vol. 38, no. 8, pp. 2201-2213, Apr. 2020.

[30] J. D. Downie, X. Liang, P. Sterlingov, N. Kaliteevskiy, and V. Ivanov, "Extension of SNR droop model for constant output power amplifier systems," in *Proc. Eur. Conf. Opt. Commun.*, Dublin, Ireland, 2019, Paper W.1.D.6.

[31] J. D. Downie *et al.*, "SNR model for generalized droop with constant output power amplifier systems and experimental measurements," *J. Lightw. Technol.*, vol. 38, no. 12, pp. 3214-3220, Jun. 2020.

[32] J.-C. Antona, A. Carbo-Meseguer, V. Letellier, "Evolution of high capacity submarine open cables," in *Proc. Asia Commun. Photon. Conf.,* Chengdu (China), 2019, Paper S4B.2.

[33] J. D. Downie *et al.*, "Experimental characterization of power efficiency for power-limited SDM submarine transmission systems" in *Proc. Eur. Conf. Opt. Commun.*, Brussels, Belgium, 2020, Paper Tu2E-5.

[34] H. Srinivas *et al.*, "Modeling and experimental measurement of power efficiency for power-limited SDM submarine transmission systems," *J. Lightw. Technol.* 2021, in press.

[35] S. Desbruslais, "Maximizing the capacity of ultra-long haul submarine systems," in *Proc. Eur. Conf. on Netw. and Opt. Commun. (NOC)*, London, UK, 2015, pp. 1-6.

[36] E. Mateo *et al.*, "Capacity limits of submarine cables," in *Proc. SubOptic,* Dubai, UAE, 2016, Paper TH1A.1.

[37] A. Bononi, J. C. Antona and P. Serena, "The generalized droop model for optical long-haul transmission systems," in Proc. *Eur. Conf. Opt. Commun.*, Brussels, Belgium, 2020, Paper We2F-1.

[38] P. Poggiolini, "The GN model of non-linear propagation in uncompensated coherent optical systems," *J. Lightw. Technol.*, vol. 30, no. 24, pp. 3857–3879, Dec. 2012.

[39] A. Carena et al. "EGN model of non-linear fiber propagation," *Opt. Express*, vol. 22, no. 13, pp. 16335--16362, Jun. 2014.

[40] P. Poggiolini, A. Carena, Y. Jiang, G. Bosco, V. Curri, and F. Forghieri, "Impact of low-OSNR operation on the performance of advanced coherent optical transmission systems," in Proc. *Eur. Conf. on Optical Commun.*, Cannes, France, 2014, Paper Mo.4.3.2.